УДК 551.32

doi: 10.31857/S2076673420010020

Поверхностные скорости и айсберговый сток ледникового купола Академии Наук на Северной Земле

© 2020 г. P. Sánchez-Gámez[1], F.J. Navarro[1*], J.A. Dowdeswell[2], E. De Andrés[1]

[1]Высшая техническая школа инженеров телекоммуникаций Мадридского политехнического университета, Мадрид, Испания;
[2]Институт полярных исследований им. Скотта, Кембриджский университет, Кембридж, Великобритания
*francisco.navarro@upm.es

Surface velocities and calving flux of the Academy of Sciences Ice Cap, Severnaya Zemlya

P. Sánchez-Gámez[1], F.J. Navarro[1*], J.A. Dowdeswell[2], E. De Andrés[1]

[1]ETSI de Telecomunicación, Universidad Politécnica de Madrid, Spain;
[2]Scott Polar Research Institute, University of Cambridge, Cambridge, United Kingdom
*francisco.navarro@upm.es

Received November 5, 2019 / Revised November 22, 2019 / Accepted December 13, 2019

Keywords: ***Arctic, calving flux, glacier calving, ice cap, ice surface velocity, Severnaya Zemlya.***

Summary

We have determined the ice-surface velocities of the Academy of Sciences Ice Cap, Severnaya Zemlya, Russian Arctic, during the period November 2016 – November 2017, using intensity offset-tracking of Sentinel-1 synthetic-aperture radar images. We used the average of 54 pairs of weekly velocities (with both images in each pair separated by a12-day period) to estimate the mean annual ice discharge from the ice cap. We got an average ice discharge for 2016–2017 of 1,93±0,12 Gt a^{-1}, which is equivalent to −0,35±0,02 m w.e. a^{-1} over the whole area of the ice cap. The difference from an estimate of ~1,4 Gt a^{-1} for 2003–2009 can be attributed to the initiation of ice-stream flow in Basin BC sometime between 2002 and 2016. Since the front position changes between both periods have been negligible, ice discharge is equivalent to calving flux. We compare our results for calving flux with those of previous studies and analyse the possible drivers of the changes observed along the last three decades. Since these changes do not appear to have responded to environmental changes, we conclude that the observed changes are likely driven by the intrinsic characteristics of the ice cap governing tidewater glacier dynamics.

Citation: Sánchez-Gámez P., Navarro F.J., Dowdeswell J.A., De Andrés E. Surface velocities and calving flux of the Academy of Science Ice Cap, Severnaya Zemlya. *Led i Sneg*. Ice and Snow. 2020. 60 (1): 19–28. [In Russian]. doi: 10.31857/S2076673420010020.

Поступила 5 ноября 2019 г. / После доработки 22 ноября 2019 г. / Принята к печати 13 декабря 2019 г.

Ключевые слова: ***айсберговый сток, Арктика, ледниковый купол, отёл ледников, поверхностная скорость движения ледника, Северная Земля.***

По 54 парам космических снимков Sentinel-1, сделанных с ноября 2016 г. по ноябрь 2017 г., определены скорости движения ледникового купола Академии Наук на Северной Земле. На этой основе оценён среднегодовой расход льда в море этого купола (1,93±0,12 Гт/год), установлены основные пути стока льда, проведено сравнение с прежними оценками.

Introduction

Frontal ablation, and in particular iceberg calving, is known to be an important mechanism of mass loss from marine-terminating Arctic glaciers [1–8], including those of the Russian Arctic [9–11]. The Russian Arctic, comprising the archipelagos of Novaya Zemlya, Severnaya Zemlya and Franz Josef Land, had a total glacierized area of 51592 km^2 in 2000–2010, of which 65% corresponded to marine-terminating glaciers [12], and an estimated total ice volume of 16 839±2205 km^3 [13]. Although the recent ice-mass losses from the Russian Arctic have been moderate, of ~11±4 Gt a^{-1} over 2003–2009 [9, 14, 15], they have been predicted to increase substantially to the end of the 21st century [16, 17]. Consequently, an accurate knowledge of the calving fluxes is key to understand and predict the evolution of the mass losses from the glaciers and ice caps of the Russian Arctic. However, the available estimates are rather scarce. Since the recent ice-mass losses in the Russian Arctic have occurred mainly in Novaya Zemlya (~80%), with Severnaya Zemlya and Franz Josef Land contributing the remaining ~20% [18, 19], the two latter regions have received comparatively lower attention. But two facts that happened in

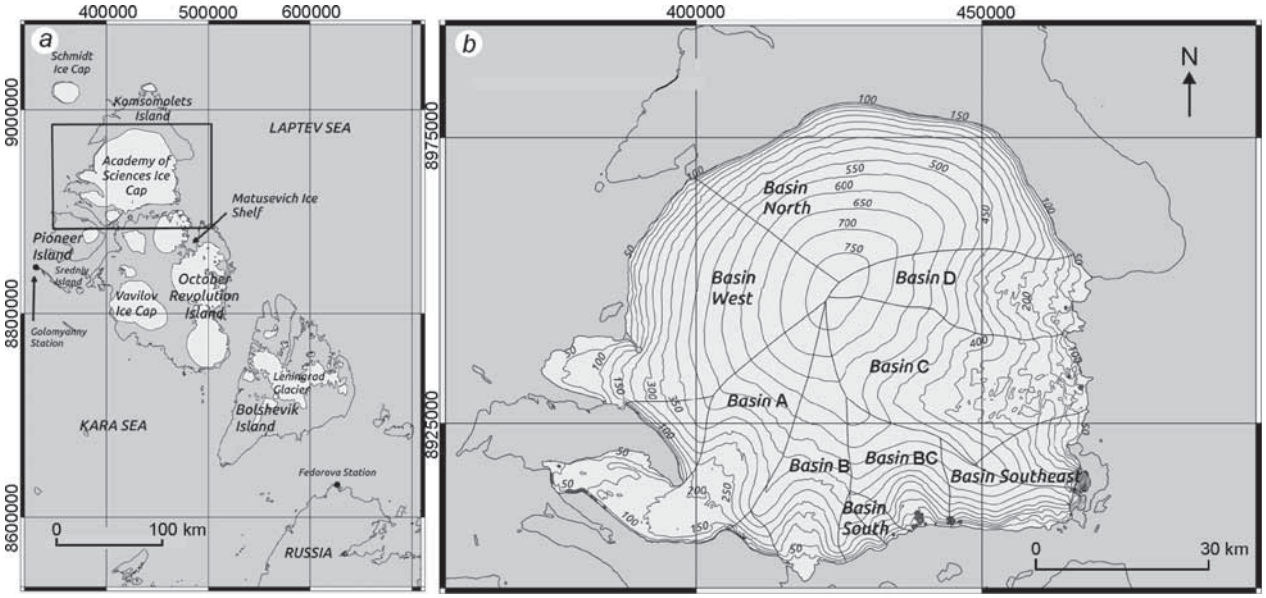

Fig. 1. Location of the Academy of Sciences Ice Cap within Severnaya Zemlya [19] (*a*), surface topography of the ice cap (contour level interval is 50 m) and ice divides defining the main basins (*b*) taken from the Randolph Glacier Inventory (RGI) version 5.0 [12].
UTM coordinates for zone 47 North are shown

Рис. 1. Местоположение ледникового купола Академии Наук на Северной Земле [19] (*a*); рельеф поверхности ледникового купола (горизонтали проведены через 50 м) и ледораздельные линии, ограничивающие основные ледосборные бассейны (*b*), показанные в соответствии с Каталогом ледников Рендольф (RGI) версии 5.0 [12].
Дана координатная сетка UTM для северной зоны 47

recent years have attracted more attention to Severnaya Zemlya. First, the collapse of the Matusevich Ice Shelf, October Revolution Island (Fig. 1, *a*), in 2012, with the subsequent accelerated thinning of the glaciers feeding the ice shelf [20]. Second, the «slow» surge of the Vavilov Ice Cap, also on October Revolution Island, in 2015 [21, 22].

There is a limited amount of earlier work on the dynamics of Severnaya Zemlya glaciers [1, 23, 24], and in particular on satellite remote-sensing studies of glacier surface velocity and ice discharge from Severnaya Zemlya [1, 9, 25]. More recently, the increased availability of Synthetic Aperture Radar (SAR) data, with higher temporal and spatial resolution, from platforms such as TerraSAR-X, PALSAR-1 and Sentinel-1, has allowed further studies [11, 22]. Focusing on the Academy of Sciences Ice Cap on Komsomolets Island, Severnaya Zemlya (see Fig. 1), which is the topic of this paper, the available surface velocity and associated calving-flux estimates differ substantially between 1988 and 2009 [1, 9], indicating large interannual to decadal variations. However, possible under- and overestimations due to limitations of the available data have been pointed out [9, 11]. This, together with the lack of studies of intra-annual (including seasonal) variations in the ice-surface velocity of this ice cap, motivated our work in a previous paper [11]. The latter paper focused on analysing the mentioned short-term variations of ice-surface velocity, and associated ice-discharge variations, though also paid attention to other aspects, such as the stress regime, the surface-elevation changes and the long-term variations in ice discharge. In the present paper, we expand the discussion by Sánchez-Gámez et al. [11], focusing on past and current calving flux estimates of the Academy of Sciences Ice Cap and on the possible drivers of the long-term variations of its calving flux.

Study site

The Academy of Sciences Ice Cap, located on Komsomolets Island, Severnaya Zemlya (see Fig. 1), is one of the largest Arctic ice caps, with an estimated area of ~5575 km^2 and volume of ~2184 km^3 [1]. Its highest elevation is of ~787 m a.s.l. (ArcticDEM, [26]) and its maximum ice thickness is of ~819 m [1]. A

large fraction (~42%) of the ice-cap margin is marine and ~50% of its bed is below sea level [1].

The climate of Severnaya Zemlya is classified as a polar desert with both low temperatures and low precipitation [9]. The atmospheric circulation is dominated by high-pressure areas over Siberia and the Arctic Ocean, and low pressure over the Barents and Kara seas [27, 28]. The climatic conditions are described with more detail in the companion paper [29], as they are more relevant for that study, focused on mass balance.

Regarding the dynamical regime of the ice cap, Dowdeswell and Williams [24] found no evidence of past surge activity within the residence time of the ice, noting that there was no evidence of any deformation of either large-scale ice structures or medial moraines. Dowdeswell et al. [1] combined ice-surface velocities from SAR interferometry of ERS tandem-phase scenes from 1995, together with ice-thickness from radio-echo sounding at 100 MHz, to calculate the calving flux from the ice cap. Moholdt et al. [9], using ICESat altimetry, together with older DEMs and velocities from Landsat imagery, calculated the geodetic mass balance and the calving flux from the Academy of Sciences Ice Cap for various periods during the last three decades. They showed that the mass balance of the ice cap has been dominated by variable ice-stream dynamics. Studies of ice-flow modelling and physical-parameter inversion are also available for the Academy of Sciences Ice Cap [30, 31].

Data and Methods

SAR data and its processing for ice surface velocities. We derived the surface velocities on the Academy of Sciences Ice Cap from Sentinel-1B SAR TOPS Interferometric Wide (IW) Level-1 Single Look Complex (SLC) images [32]. The resolution when operating in this mode is 5 of and 20 m in the range and azimuth directions, respectively. We used the vertical transmit and vertical receive (VV) channel, which is best suited for retrieval of ice motion [33]. We processed 54 weekly pairs of SAR images, from November 2016 to November 2017, with 12-day separation between the images in each pair. Additional details can be found in [11].

We used the intensity offset-tracking algorithm GAMMA software for processing the Sentinel-1 SAR acquisitions [34, 35]. For co-registration of the Sentinel-1 TOPS mode images, we used the ArcticDEM mosaic release 6 [26]. After full co-registration is achieved, deramping of the SLC images for correcting the azimuth phase ramp is required to apply oversampling in the offset-tracking procedures [35]. Once these steps are completed, the offset-tracking technique is the usual one for stripmap mode scenes [34, 36]. We used a matching window of 320 × 64 pixels (1200 × 1280 m) in range and azimuth directions, respectively, with an oversampling factor of two for improving the tracking results [34]. The resolution of the final velocity map was 130 × 105 m in range and azimuth directions. The geocoding was completed using the ArcticDEM mosaic product. Errors in surface velocity were estimated by analysing the performance of the algorithm on ice-free ground on Komsomolets Island under the hypothesis that the error of the offset tracking technique on bare ground should be close to zero. The combined (range and azimuth) root-mean-square error in the magnitude of the ice-surface velocity was ~0,024 m d^{-1} (~8,75 m a^{-1}).

Ice thickness data from radio-echo sounding. Ice-thickness data were derived from radio-echo sounding measurements in spring 1997 using a 100 MHz radar system [1]. The mean crossing-point error in ice-thickness measurements was 10,5 m.

Dynamic ice discharge and calving flux. We here use the term calving flux to denote the ice discharge calculated through a flux gate close to the calving front minus the mass flux involved in front position changes [37]. In our case study, spanning the period from November 2016 to November 2017, glacier terminus position changes have been negligible, so calving flux and ice discharge are equivalent. We will most often use the term calving flux, for consistency with previous studies [1, 9].

For tidewater glaciers, ice discharge is ideally calculated through flux gates as close as possible to the calving fronts, while for floating ice tongues or ice shelves it is usually calculated at the grounding line. There is some evidence from both ice-penetrating radar data collected in 1997 and earlier investigations by Russian scientists that small areas of the ice-cap margin at the seaward end of the ice streams of the Academy of Sciences Ice Cap may be floating or close to floatation [1]. However, we calculated ice discharge at flux gates located within ca. 1,5–3 km of the calving front, where ice is grounded. Therefore,

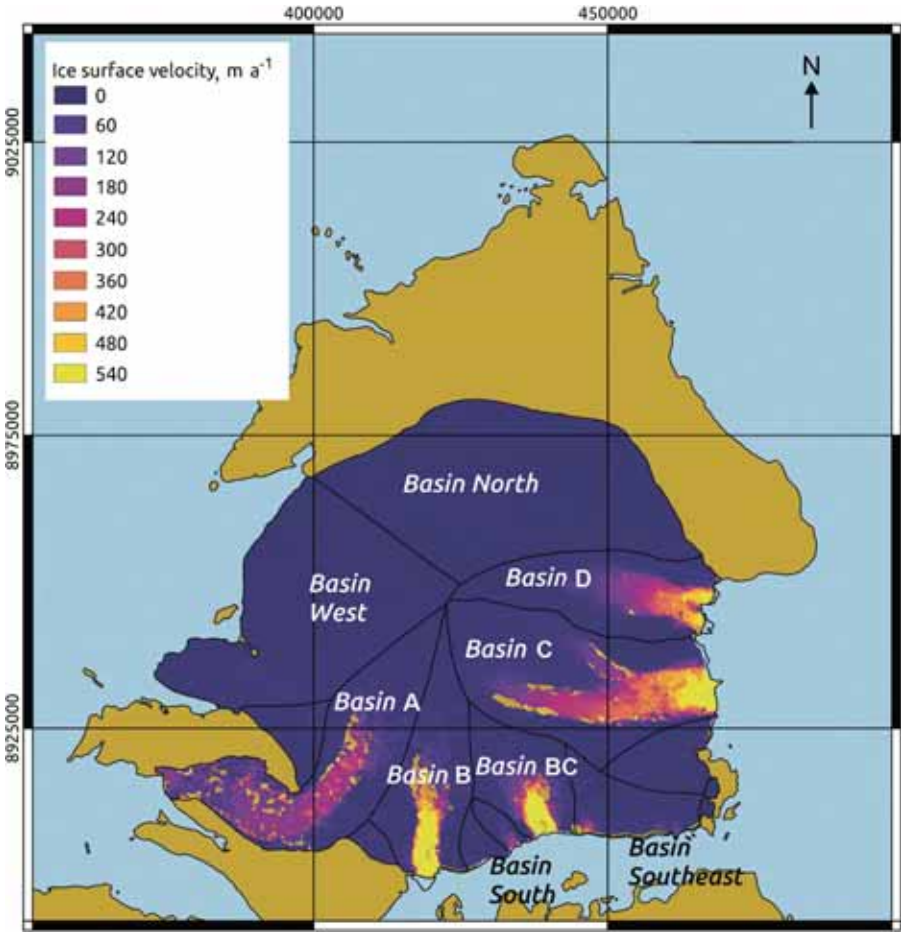

Fig. 2. Surface velocities for the drainage basins of the Academy of Sciences Ice Cap, corresponding to the Sentinel-1 SAR image pair acquired on 6 and 18 March 2017. Brown colour indicates ice-free land areas. The maximum velocities are 1200 m a^{-1} for basins B and BC, 1100 m a^{-1} for Basin C and 750 m a^{-1} for Basin D

Рис. 2. Поверхностные скорости движения в ледосборных бассейнах ледникового купола Академии Наук, соответствующие паре изображений SAR Sentinel-1, полученных 6 и 18 марта 2017 г. Коричневым цветом обозначены свободные ото льда участки суши. Максимальные скорости достигают 1200 м/год в бассейнах B и BC, 1100 м/год в бассейне C и 750 м/год в бассейне D

ice discharge can be calculated as mass flux per unit time across a given vertical surface S, approximated using area bins as

$$\phi = \int_S \rho v \cdot dS \approx \sum_i \rho L_i H_i f v_i \cos\gamma_i, \quad (1)$$

where ρ is the ice density, L_i and H_i are respectively the width and thickness of an area bin, f is the ratio of surface to depth-averaged velocity, v_i is the magnitude of surface velocity and γ_i is the angle between the surface-velocity vector and the direction normal to the local flux gate for the bin under consideration. In general, it is assumed that f ranges between 0.8 and 1 [38]. Normally, tidewater-glacier velocity at the terminus is dominated by basal sliding, making f close to unity. Following [39], we took $f = 0.93 \pm 0.05$, assuming that all tidewater glaciers on the Academy of Sciences Ice Cap have a large component of basal motion. For ice density, we assumed $\rho = 900 \pm 17$ kg m^{-3}. Our flux gates span the whole frontal area of each marine-terminating glacier basin. Each flux gate was divided into small bins of 30 m width. The ice thickness for each bin was calculated by interpolating the ice-thickness data of Dowdeswell et al. [1], and was corrected for surface-elevation changes between 2004 and 2016 from the comparison of ICESat and ArcticDEM strip elevation datasets (see companion paper [20]). The velocity vector orientations were calculated with respect to the vector normal to each flux-gate bin. Errors in ice discharge were estimated following [7], applying error propagation to Equation 1.

Results

Ice cap surface velocity. The surface velocities inferred from the Sentinel-1 SAR images are shown in Fig. 2. The marine-terminating drainage basins B, BC, C and D show zones of ice-stream-like flow with high velocities, while Basin A also shows a well-defined zone of lower, but relatively high velocities. The surface-velocity fields of all major ice streams, except A, show a similar pattern. Velocities become prominent where ice flow converges from the upper

Table 1. **Area, flux gate main characteristics and mean annual (November 2016 – November 2017) calving fluxes for the marine-terminating drainage basins of the Academy of Sciences Ice Cap shown in Fig. 2. The totals are shown in the last row**
Таблица 1. **Площади, основные характеристики и среднегодовые (ноябрь 2016 – ноябрь 2017 гг.) расходы льда на айсберги ледниковых бассейнов купола Академии Наук, заканчивающихся в море и показанных на рис. 2. В последней строке даны итоговые значения**

Drainage basin	Basin area, km^2	Flux gate length, m	Flux gate mean thickness, m	Flux gate mean surface velocity, m a^{-1}	Calving flux, Gt a^{-1}
West	1033	62 821	174	6	0,06±0,03
A	707	7274	251	19	0,03±0,01
B	413	5788	83	441	0,18±0,03
South	47	14 107	121	28	0,04±0,02
BC	276	6820	184	384	0,41±0,05
Southeast	359	3740	164	15	0,08±0,04
C	829	10 594	223	344	0,69±0,07
D	475	10 820	171	280	0,44±0,05
Total	**4139**	**155 264**	**166**	**88**	**1,93±0,12**

accumulation areas and increase to a maximum at the marine termini. We also calculated the mean annual velocities at the flux gates of all marine-terminating basins, by averaging the 54 pairs of weekly-spaced Sentinel-1 SAR velocities available between November 2016 and November 2017. These annual-averaged velocities, shown in Table 1, were later used to compute the ice discharge.

Calving flux. The calving flux calculated for each individual basin of the Academy of Sciences Ice Cap, for the period November 2016 – November 2017, is presented in Table 1. The largest contributors are the southern (B and BC) and eastern (C and D) basins, where the fastest ice streams are located. The total calving flux from the ice cap amounts to 1.93±0.12 Gt a^{-1}, which is equivalent to −0.35±0.02 m w.e. a^{-1} over the whole area of the ice cap.

Discussion

Calving flux and its intra-annual variability. Ice Streams A, B, C and D were identified in the earlier observations by Dowdeswell et al. [1] and Moholdt et al. [9], but Ice Stream BC, which is currently the third largest contributor to total calving flux, was first noted in our study [11]. Our data thus indicate that fast ice-stream flow was initiated in this basin after the period covered by the two earlier studies and before our study period began in 2017. Sánchez-Gámez et al. [11] additionally compared a Landsat-7 image of July 2002 with a Sentinel-2 image from March 2016, and fast flow did not appear in the former, while it was clearly evident in the latter. Therefore, ice stream flow in Basin BC was initiated after 2002, and before 2016.

The calving flux values shown in Table 1 are annual averages for the period November 2016 – November 2017, based on weekly observations along the entire year, and thus are not affected by seasonal or other shorter-term intra-annual variations. Sánchez-Gámez et al. [11] have analysed these intra-annual variations, which, for certain basins, can reach peak-to-peak variations up to ~40% with respect to the mean annual velocity. This indicates that large errors could be incurred if the ice velocities calculated at a particular snapshot in time were extrapolated to calculate the calving flux for the whole year.

Interannual variability of calving flux. There are available some calving flux estimates for the Academy of Sciences Ice Cap, derived using different techniques, and corresponding to various periods within the last ~30 years, some of which partly overlap. Dowdeswell et al. [1] calculated the calving flux for September/December 1995 from SAR interferometry, whereas Moholdt et al. [9] did it for the period June 2000 – August 2002 using image-matching of Landsat scenes. Moholdt et al. [9] also calculated the calving flux for the periods 1988–2006 and 2003–2009, using in these cases an indirect way, subtracting from the geodetic mass balance (calculated from DEM differencing assuming Sorge's law [40]) an estimate of the climatic mass balance. The latter was based on the assumption that Basin North (basins North and West in our study) is an analogue for the climatic mass balance of the entire ice cap [9]. The justification for this

Table 2. **Calving fluxes estimated for the drainage basins of the Academy of Sciences Ice Cap for various periods. Basin «North» here groups our basins North and West, and «Others» groups our basins South, BC and Southeast. These names have been used for compatibility with [9]**
Таблица 2. **Расходы льда на айсберги, оценённые за разные периоды для ледосборных бассейнов ледникового купола Академии Наук. Здесь бассейн «North» включает в себя наши бассейны North и West, а бассейн «Others» – наши бассейны South, BC и Southeast. Эти названия были использованы для возможности сравнения с данными работы [9]**

Drainage Basin	Dowdeswell et al. [1]		Moholdt et al. [9]		This study
	1995 Gt a^{-1}	1988–2006 Gt a^{-1}	2000–2002 Gt a^{-1}	2003–2009 Gt a^{-1}	2016/2017 Gt a^{-1}
Basin North	~0	~0	~0	~0	0,06±0,03
A	~0	~0	~0	~0	0,03±0,01
B	0,03	0,5	0,3	0,1	0,18±0,03
C	0,37	1,9	1,9	0,7	0,69±0,07
D	0,12	0,7	~0,7	0,5	0,44±0,05
Others	~0,1	~0,1	~0,1	~0,1	0,53±0,07
Ice cap total	**0,6**	**3,2**	**~3,0**	**1,4**	**1,93±0,12**

assumption is that the northern part of the ice cap is land-terminating, so its climatic and geodetic mass balances are equal; on the other hand, the western part of the ice cap, although marine-terminating, is dynamically inactive with no significant calving losses. Extrapolating the estimated climatic mass balance to the rest of the ice cap leads to a near-zero climatic mass balance for the entire Academy of Sciences Ice Cap. We have made a similar assumption in the companion paper [20], where we discuss other pieces of evidence supporting this assumption.

The available calving flux estimates are shown in Table 2. There are significant variations along the period analysed, although the calving flux in the last decade seems more stable than in previous decades (see Table 2). It is important to remark that the difference of ~0,5 Gt a^{-1} between the estimates for 2003–2009 and 2016–2017 is almost entirely attributed to the recent initiation of fast flow in Basin BC [11], which currently accounts for 0.41 ± 0.05 Gt a^{-1} (see Table 1). The lowest calving flux estimate, of 0.6 Gt a^{-1} for 1995, could have been underestimated, as discussed by Moholdt et al. [9] and Sánchez-Gámez et al. [11]. The main potential shortcoming of the indirect estimates of calving flux for 1988–2006 and 2003–2009 is the assumption of Sorge's law in the conversion from volume changes to mass changes. The analysis by Opel et al. [41] of the deep ice core taken in 1999–2001 at the summit of the Academy of Sciences Ice Cap found a strong increase in melt-layer content at the beginning of the 20th century, which remained at a high level until about 1970 and then decreased markedly until 1998. As the amount of melt layers in ice cores is a proxy for the summer warmth at the ice-cap surface [42], these large temporal variations in melt-layer content indicate that the assumption in Sorge's law of an absence of temporal change in firn thickness or density is not suitable for the Academy of Sciences Ice Cap. Further evidence is provided by the modelling experiments on the neighbouring Vavilov Ice Cap on October Revolution Island, Severnaya Zemlya [43, 44]. Even so, the associated uncertainty cannot justify the large differences in calving flux observed between the various periods shown in Table 2. For the calving flux estimates based on data for particular snapshots in time, the period in the year when the observations were made can neither explain such large differences, considering the magnitude of the seasonal and intra-annual variability in surface velocities analysed by Sánchez-Gámez et al. [11]. Hence the need to search for drivers of the large differences in calving flux observed over the last three decades.

Drivers of the observed long-term changes in calving flux. Increasing summer air temperatures may drive an increase of calving flux, through its influence on surface melting and drainage of meltwater to the glacier bed, enhancing bed lubrication and basal sliding [45]. However, such accelerations in velocity are mostly short-lived and do not contribute to increased calving [46]. Air temperatures could still play a role if they had an influence on sea-ice or ice mélange concentration, as these are known to affect calving, especially when glaciers are confined in fjords [47, 48]. However, the possible effects of sea-ice cover on the dynamics and calving flux of the Academy of Sciences Ice Cap are expected to be weak, because their marine termini are not confined

in fjords where sea ice or ice mélange could form, be retained and exert a significant backpressure. Moreover, the seas surrounding Severnaya Zemlya are characterized by relatively thin first-year ice, as in this region new ice is typically produced and soon moved away by the oceanic currents that flow northwards past the archipelago [49]. However, Sharov and Tyukavina [25] pointed out that medium-term (from decadal to semi-centennial) changes in glacier volumes on Severnaya Zemlya were linked to the extent and duration of sea-ice cover nearby, so that slow-moving maritime ice caps would grow when the sea-ice cover in adjacent waters was small, and thin when the sea-ice cover consolidated. This, however, would apply in our case study only to the slow-moving basins West and A. More generally we did not find any clear relationship between summer (June–July–August) average temperature and calving flux, or between sea-ice concentration and calving flux, which could explain the observed long-term changes in calving flux [11]. In fact, the highest calving fluxes corresponded to the period 1988–2006, which had, overall, lower air temperatures and larger late September sea-ice extent than the periods 2003–2009 and 2016–2017 [11]. The calving flux in 2003–2009 was lower than that of 2016–2017, and mean summer temperatures during 2003–2009 (~0,8 °C on average) were higher than that of summer 2017 (−0.2 °C). The mean late September sea-ice extent was also higher on average for 2003–2009 compared with 2016–2017 [11]. Only for the lowest calving flux estimate, which corresponds to particular snapshots in time (September and November 1995), did we find that the sea-ice extent in late September was larger than those of the preceding and following years [11]. The summer before our SAR image acquisitions (2016) was relatively warm (mean summer air temperature of 1.2 °C), but was followed by a marked drop in temperature, to – 0.2 °C in summer 2017 [11]. However, the sea surrounding northern Severnaya Zemlya was virtually ice free at the end of September 2017 [11].

In the absence of a clear climate-related driver for the large interannual changes in calving flux observed during the last three decades, we are inclined to associate the observed dynamic instabilities with intrinsic characteristics within the Academy of Sciences Ice Cap, as suggested by Moholdt et al. [9]. One of the characteristics that could influence long-term variations in terminus position and calving fluxes is the complex geometry of the subglacial and seabed topography in the terminal zones of the eastern basins (C and D) [1]. The variations of flux could be associated with changes in floatation conditions [50]. The floating or near-floating state of these marginal zones has been suggested through various lines of evidence, such as the very low ice-surface gradients, the strong radar returns from the ice-cap bed in several areas at the margin of the ice streams, and the large numbers of tabular icebergs observed near their margins [1].

Conclusions

The following main conclusions can be drawn from our analysis:

1. During the period November 2016 – November 2017, the marine-terminating margins of the Academy of Sciences Ice Cap remained nearly stable, so that ice discharge and calving flux are equivalent in our study, at 1.93±0.12 Gt a^{-1}. This is equivalent to −0.35±0.02 m w.e. a^{-1} over the whole area of the ice cap.

2. The difference of ~0.5 Gt a^{-1} between our estimate and that of Moholdt et al. [9] for 2003–2009, of ~1.4 Gt a^{-1}, can be attributed to the initiation, sometime between 2002 and 2016, of ice stream flow in Basin BC, whose current calving flux is estimated to be of 0.41±0.05 Gt a^{-1}.

3. The long-term (from interannual to interdecadal) variations of calving flux during the last three decades have been large, at between 0.6 and 3.2 Gt a^{-1}.

4. The lack of clear environmental drivers for the observed long-term changes of calving flux suggests that these variations are an expression of dynamic instability, likely associated with intrinsic characteristics of the ice cap. We suggest that this instability could be caused by the long-term changes in floatation conditions associated with the complex geometry of the subglacial and seabed topography in the terminal zones of the fast-flowing eastern basins (B and C).

5. Given that the climatic mass balance has remained close to zero over the last four decades, in spite of regional warming (see the companion paper [20]), the total mass balance of the ice cap has been driven mainly by calving flux.

Acknowledgments. This study has received funding from the European Union's Horizon 2020 research and innovation programme under grant agreement No 727890 and from Agencia Estatal de Investig-

ación under grant CTM2017-84441-R of the Spanish Estate Plan for R & D. The radio-echo sounding campaign was funded by grants GR3/9958 and GST/02/2195 to JAD from the UK Natural Environment Research Council. Copernicus Sentinel data 2016–2017 were processed by ESA.

Расширенный реферат

Определены поверхностные скорости движения ледникового купола Академии Наук на о. Комсомолец (архипелаг Северная Земля в Российской Арктике) в течение периода с ноября 2016 г. по ноябрь 2017 г. Для этого использован метод оценки смещения элементов с разной интенсивностью отражения на разновременных радарных изображениях, полученных группировкой спутников Sentinel-1. Получены 54 пары недельных скоростей (по двум изображениям в каждой паре, разделённым 12-дневным периодом). Общая (по дальности и азимуту) среднеквадратичная ошибка в определении скорости движения поверхности льда составила около 0,024 м/день (≈8,75 м/год). Для оценки среднегодового расхода льда в море этого ледникового купола использовано среднее значение этих 54-недельных скоростей. По нашим оценкам, средний расход льда за 2016–2017 гг. составил 1,93±0,12 Гт/год, что эквивалентно потерям −0,35±0,02 м вод. экв. в год по всей площади ледникового купола. Основной сброс льда в море формируют те выводные ледники, которые дренируют купол в южном и восточном направлениях. Расхождение с прежней оценкой расхода льда этого купола в море в ~1,4 Гт/год, приведённой для 2003–2009 гг. другими авторами, может быть объяснено активизацией выводного ледника в ледосборном бассейне ВС, которая произошла где-то между 2002 и 2016 гг. Поскольку изменения положения фронтов выводных ледников между обоими периодами были незначительными, полученные значения расходов льда через поперечные сечения в краевых частях эквивалентны айсберговому стоку. Выполнено сравнение наших результатов оценок расхода льда в море с результатами предыдущих исследований и проанализированы возможные движущие силы тех изменений, которые наблюдаются в течение последних трёх десятилетий. Поскольку эти изменения, по-видимому, не были реакцией на изменения окружающей среды, авторы пришли к выводу, что наблюдаемые изменения, вероятно, обусловлены внутренними характеристиками ледникового купола, которые регулируют динамику его выводных ледников, достигающих моря. В частности, предполагается, что эта динамическая нестабильность может быть вызвана долгосрочными изменениями условий всплывания, связанными со сложной геометрией рельефа подледникового ложа и прилегающего морского дна в краевых зонах быстротекущих выводных ледников с восточной стороны купола.

References

1. *Dowdeswell J., Bassford R., Gorman M., Williams M., Glazovsky A., Macheret Y., Shepherd A., Vasilenko Y., Savatyuguin L., Hubberten H., Miller H.* Form and flow of the Academy of Sciences Ice Cap, Severnaya Zemlya, Russian High Arctic. Journ. of Geophys. Research. 2002, 107: 1–16. doi: 10.1029/2000jb000129.
2. *Błaszczyk M., Jania J., Hagen J.* Tidewater glaciers of Svalbard: recent changes and estimates of calving fluxes. Polish Polar Research. 2009, 30 (2): 85–142.
3. *Bolch T., Sandberg Sørensen L., Simonsen S.B., Mölg N., Machguth H., Rastner P., Paul F.* Mass loss of Greenland's glaciers and ice caps 2003–2008 revealed from ICESat laser altimetry data. Geophys. Research Letters. 2013, 40: 875–881. doi: 10.1002/grl.50270.
4. *Burgess E., Forster R., Larsen C.* Flow velocities of Alaskan glaciers. Nature Communications. 2013, 4: 2146. doi: 10.1038/ncomms3146.
5. *McNabb R., Hock R., Huss M.* Variations in Alaska tidewater glacier frontal ablation, 1985–2013. Journ. of Geophys. Research. 2015, 120 (1): 120–136. doi: 10.1002/2014jf003276.
6. *Sánchez-Gámez P., Navarro F.J.* Glacier Surface Velocity Retrieval Using D-InSAR and Offset Tracking Techniques Applied to Ascending and Descending Passes of Sentinel-1 Data for Southern Ellesmere Ice Caps, Canadian Arctic. Remote Sensing. 2017, 9 (5): 442. doi: 10.3390/rs9050442.
7. *Sánchez-Gámez P., Navarro F.J.* Ice discharge error estimates using different cross-sectional area approaches: a case study for the Canadian High Arctic, 2016/17. Journ. of Glaciology. 2018, 64 (246): 595–608. doi: 10.1017/jog.2018.48.
8. *De Andrés E., Otero J., Navarro F., Promińska J., Lapazaran J., Walczowski W.* A two-dimensional glacier–fjord coupled model applied to estimate submarine melt rates and front position changes of Hansbreen,

Svalbard. Journ. of Glaciology. 2018, 64 (247): 745–758, doi: 10.1017/jog.2018.61.

9. *Moholdt G., Heid T., Benham T., Dowdeswell J.* Dynamic instability of marine-terminating glacier basins of Academy of Sciences Ice Cap, Russian High Arctic. Annals of Glaciology. 2012, 53: 193–201. doi: 10.3189/2012aog60a117.
10. *Melkonian A., Willis M., Pritchard M., Stewart A.* Recent changes in glacier velocities and thinning at Novaya Zemlya. Remote Sensing of Environment. 2016, 174: 244–257. doi: 10.1016/j.rse.2015.11.001.
11. *Sánchez-Gámez P., Navarro F., Benham T., Glazovsky A., Bassford R., Dowdeswell J.* Intra- and inter-annual variability in dynamic discharge from the Academy of Sciences Ice Cap, Severnaya Zemlya, Russian Arctic, and its role in modulating mass balance. Journ. of Glaciology. 2019, 65 (253): 780–797. doi: 10.1017/jog.2019.58.
12. *Pfeffer W., Anthony A., Bliss A., Bolch T., Cogley G., Gardner A., Ove Hagen J., Hock R., Kaser G., Kienholz C., Miles E., Moholdt G., Mölg N., Paul F., Radić V., Rastner P., Raup B., Rich J., Sharp M., The Randolph Consortium*. The Randolph Glacier Inventory: a globally complete inventory of glaciers. Journ. of Glaciology. 2014, 60: 537–552. doi: 10.3189/2014JoG13J176.
13. *Huss M., Farinotti D.* Distributed ice thickness and volume of all glaciers around the globe. Journ. of Geophys. Research: Earth Surface. 2012, 117: 1–10. doi: 10.1029/2012jf002523.
14. *Matsuo K., Heki K.* Current ice loss in small glacier systems of the Arctic islands (Iceland, Svalbard, and the Russian High Arctic) from satellite gravimetry. Terrestrial Atmospheric and Oceanic Sciences. 2013, 24: 657–670. doi: 10.3319/tao.2013.02.22.01(tibxs).
15. *Gardner A., Moholdt G., Cogley J., Wouters B., Arendt A., Wahr J., Berthier E., Hock R., Pfeffer W., Kaser G., Ligtenberg S., Bolch T., Sharp M., Ove Hagen J., van den Broeke M., Paul F.* A reconciled estimate of glacier contributions to sea level rise: 2003 to 2009. Science. 2013, 340: 852–857. doi: 10.1126/science.1234532.
16. *Radić V., Bliss A., Beedlow C., Hock R., Miles E., Cogley G.* Regional and global projections of twenty-first century glacier mass changes in response to climate scenarios from global climate models. Climate Dynamics. 2013, 42: 37–58. doi: 10.1007/s00382-013-1719-7.
17. *Huss M., Hock R.* A new model for global glacier change and sea-level rise. Frontiers in Earth Science. 2015, 3: 1–22. doi: 10.3389/feart.2015.00054.
18. *Moholdt G., Wouters B., Gardner A.* Recent mass changes of glaciers in the Russian High Arctic. Geophys. Research Letters. 2012, 39: 1–5. doi: 10.1029/2012gl051466.
19. *Wessel P., Smith W.* A global, self-consistent, hierarchical, high-resolution shoreline database. Journ. of Geophys. Research. 1996, 101: 8741–8743. doi: 10.1029/96JB00104.
20. *Willis M., Melkonian A., Pritchard M.* Outlet glacier response to the 2012 collapse of the Matusevich Ice Shelf, Severnaya Zemlya, Russian Arctic. Journ. of Geophys. Research: Earth Surface. 2015, 120: 2040–2055. doi: 10.1002/2015jf003544.
21. *Glazovsky A., Bushueva I., Nosenko G.* 'Slow' surge of the Vavilov Ice Cap, Severnaya Zemlya. Proc. of the IASC Workshop on the Dynamics and Mass Balance of Arctic Glaciers, Obergurgl, Austria, 23–25 March 2015: 17–18.
22. *Strozzi T., Paul F., Wiesmann A., Schellenberger T., Kääb A.* Circum-Arctic changes in the flow of glaciers and ice caps from satellite SAR data between the 1990s and 2017. Remote Sensing. 2017, 9: 947. doi: 10.3390/rs9090947.
23. *Dowdeswell J., Williams M.* Surge-type glaciers in the Russian High Arctic identified from digital satellite imagery. Journ. of Glaciology. 1997, 43: 489–494. doi: 10.3189/S0022143000035097.
24. *Dowdeswell J., Dowdeswell E., Williams M., Glazovsky A.* The glaciology of the Russian High Arctic from Landsat imagery. U.S. Geological Survey Professional Paper. 2010, 1386-F: 94–125.
25. *Sharov A., Tyukavina A.* Mapping and interpreting glacier changes in Severnaya Zemlya with the aid of differential interferometry and altimetry. Proc. of Fringe 2009 Workshop, Frascati, Italy, 30 November – 4 December 2009, ESA SP-677: 8 p.
26. *Noh M.J., Howat I., Porter C., Willis M., Morin P.* Arctic Digital Elevation Models (DEMs) generated by Surface Extraction from TIN-Based Search space Minimization (SETSM) algorithm from RPCs-based Imagery. AGU Fall Meeting Abstracts. 2016, EP24C-07.
27. *Alexandrov E., Radionov V., Svyashchennikov P.* Snow cover thickness and its measurement in Barents and Kara seas. In: Research of climate change and interaction processes between ocean and atmosphere in polar regions. Trudy of the Arctic and Antarctic Research Institute. St. Petersburg, 2003, 446: 99–118. [In Russian].
28. *Bolshiyanov D., Makeyev V. Arkhipelag Severnaya Zemlya: Oledeneniye, Istoriya Razvitiya Prirodnoy Sredy.* Severnaya Zemlya Archipelago: Glaciation and Historical Development of the Natural Environment. St. Petersburg: Gidrometeoizdat, 1995: 216 p. [In Russian].
29. *Navarro F.J., Sánchez-Gámez P., Glazovsky A.F., Recio-Blitz C.* Surface-elevation changes and mass balance of the Academy of Sciences Ice Cap, Severnaya Zemlya. *Led i Sneg*. Ice and Snow. 2020, 60 (1): 29–41. doi: 10.31857/S2076673420010021
30. *Konovalov Y.* Inversion for basal friction coefficients with a two-dimensional flow line model using Tik-

honov regularization. Research in Geophysics. 2012, 2: 11. doi: 10.4081/rg.2012.e11.
31. *Konovalov Y., Nagornov O.* Two-dimensional prognostic experiments for fast-flowing ice streams from the Academy of Sciences Ice Cap. Journ. of Physics. Conference Series. 2017, 788: 012051. doi: 10.1088/1742-6596/788/1/012051.
32. *Zan F.D., Guarnieri A.M.* TOPSAR: Terrain observation by progressive scans. IEEE Transactions on Geoscience and Remote Sensing. 2006, 44 (9): 2352–2360. doi: 10.1109/tgrs.2006.873853.
33. *Nagler T., Rott H., Hetzenecker M., Wuite J., Potin P.* The Sentinel-1 mission: new opportunities for ice sheet observations. Remote Sensing. 2015, 7: 9371–9389. doi: 10.3390/rs70709371.
34. *Strozzi T., Luckman A., Murray T., Wegmuller U., Werner C.* Glacier motion estimation using SAR offset-tracking procedures. IEEE Transactions on Geoscience and Remote Sensing. 2002, 40: 2384–2391. doi: 10.1109/tgrs.2002.805079.
35. *Wegmüller U., Werner, C., Strozzi, T., Wiesmann, A., Othmar, F., Santoro, M.* Sentinel-1 support in the GAMMA software. Proceedings of the FRINGE'15: Advances in the Science and Applications of SAR Interferometry and Sentinel-1 InSAR Workshop, Frascati, Italy. 2015: 23–27.
36. *Werner C., Wegmüller U., Strozzi T., Wiesmann A.* Precision estimation of local offsets between pairs of SAR SLCs and detected SAR images. 2005 IEEE Intern. Geoscience and Remote Sensing Symposium (IGARSS'05). IEEE Intern. Proceedings. 2005, 7: 4803–4805. doi: 10.1109/IGARSS.2005.1526747.
37. *Cogley, J., Hock R., Rasmussen L., Arendt A., Bauder A., Braithwaite R., Jansson P., Kaser G., Möller M., Nicholson L., Zemp M.* Glossary of glacier mass balance and related terms. IHP-VII Technical Documents in Hydrology No. 86, IACS Contribution No. 2, UNESCO-IHP, Paris, 2011: 114 p. doi: 10.1017/S0032247411000805.
38. *Cuffey K., Paterson S.* The Physics of Glaciers, 4th Ed. Oxford: Butterworth-Heinemann, 2010: 704 p.
39. *Vijay S., Braun M.* Seasonal and interannual variability of Columbia Glacier, Alaska (2011–2016): Ice velocity, mass flux, surface elevation and front position. Remote Sensing. 2017, 9: 635. doi: 10.3390/rs9060635.
40. *Bader H.* Sorge's law of densification of snow on high polar glaciers. Journ. of Glaciology. 1954, 2: 319–323. doi: 10.3189/s0022143000025144.
41. *Opel T., Fritzsche D., Meyer H., Schütt R., Weiler K., Ruth U., Wilhelms F., Fischer H.* 115 year ice-core data from Akademii Nauk Ice Cap, Severnaya Zemlya: high-resolution record of Eurasian Arctic climate change. Journ. of Glaciology. 2009, 55: 21–31. doi: 10.3189/002214309788609029.
42. *Koerner R.* Devon Island Ice Cap: Core stratigraphy and paleoclimate. Science. 1977, 196: 15–18. doi: 10.2307/1744032.
43. *Bassford R., Siegert M., Dowdeswell J.* Quantifying the mass balance of Ice Caps on Severnaya Zemlya, Russian high Arctic. II: modeling the flow of the Vavilov Ice Cap under the present climate. Arctic, Antarctic, and Alpine Research. 2006, 38: 13–20. doi: 10.1657/1523-0430(2006)038[0013:qtmboi]2.0.co;2.
44. *Bassford R., Siegert M., Dowdeswell J., Oerlemans J., Glazovsky A., Macheret Y.* Quantifying the mass balance of Ice Caps on Severnaya Zemlya, Russian high Arctic. I: climate and mass balance of the Vavilov Ice Cap. Arctic, Antarctic, and Alpine Research. 2006, 38: 1–12. doi: 10.1657/1523-0430(2006)038[0001:qtmboi]2.0.co;2.
45. *Zwally H.J.* Surface melt-induced acceleration of Greenland Ice-Sheet Flow. Science. 2002, 297 (5579): 218–222. doi: 10.1126/science.1072708.
46. *Sundal A.V. and 5 others.* Melt-induced speed-up of Greenland Ice Sheet offset by efficient subglacial drainage. Nature. 2011, 469 (7331): 521–524. doi: 10.1038/nature09740.
47. *Moon T., Joughin I., Smith B.* Seasonal to multiyear variability of glacier surface velocity, terminus position, and sea ice/ice mélange in northwest Greenland. Journ. of Geophys. Research. Earth. 2015, 120: 818–833. doi: 10.1002/2015jf003494.
48. *Otero J., Navarro F., Lapazaran J., Welty E., Puczko D., Finkelnburg R.* Modeling the controls on the front position of a tidewater glacier in Svalbard. Frontiers in Earth Science. 2017, 5:1–11. doi: 10.3389/feart.2017.00029.
49. *Serreze M.C., Barry R.G.* The Arctic Climate System. Cambridge: Cambridge University Press, 2005: 385 p.
50. *Howat I., Joughin I., Scambos T.* Rapid changes in ice discharge from Greenland outlet glaciers. Science. 2007, 315: 1559–1561. doi: 10.1126/science.1138478.